ELSEVIER

Physica A 239 (1997) 276–285

PHYSICA A

Some progress in the lattice Boltzmann method: Reynolds number enhancement in simulations

Xiaoyi He[a,b,c], Li-Shi Luo[c,d,e,*], Micah Dembo[b]

[a] *Center for Nonlinear Studies, MS-B258, Los Alamos National Laboratory, Los Alamos, NM 87545, USA*

[b] *Theoretical Biology and Biophysics Group T-10, MS-K710, Theoretical Division, Los Alamos National Laboratory, Los Alamos, NM 87545, USA*

[c] *Complex Systems Group T-13, MS-B213, Theoretical Division, Los Alamos National Laboratory, Los Alamos, NM 87545, USA*

[d] *Computational Science Methods Group XCM, MS-F645, Applied Theoretical & Computational Physics Division, Los Alamos National Laboratory, Los Alamos, NM 87545, USA*

[e] *ICASE, Mail Stop 403, NASA Langley Research Center, Bldg 1298, 6 North Dryden St., Hampton, VA 23681-0001, USA*

Abstract

A newly proposed lattice Boltzmann algorithm is used to simulate flows with high Reynolds number. The new algorithm is not limited by the lattice Reynolds number which constrains all previous lattice Boltzmann models. Not only is the Reynolds number enhanced in the simulation using the new algorithm, but also is the numerical stability improved significantly. Numerical simulations of the flow in a 2-D symmetrical sudden expansion were conducted to demonstrate the effectiveness of the new algorithm.

Keywords: Lattice Boltzmann method; High Reynolds number simulation; Nonuniform mesh grids; Flow in 2-D symmetric channel with sudden expansion

1. Introduction

Recently, we proposed a new algorithm of the lattice Boltzmann equation (LBE) which can be straightforwardly implemented on arbitrary, nonuniform mesh grids [1]. With arbitrary and nonuniform meshes, the computational efficiency of the LBE method is much enhanced. The system size of the nonuniform mesh grids in the new LBE algorithm is comparable to that in other conventional methods such as the finite difference

* Correspondence address: ICASE, Mail stop 403, NASA Langley Research Centre, Bldg 1298, 6 North Dryden St., Hampton, VA 23681-0001, USA. E-mail: luo@icase.edu

PII S0378-4371(96)00486-4

or the finite element method, yet the LBE method is much less computationally intensive on each mesh grid point than them. This advancement allows the LBE method to be a superior computational tool compared with other conventional methods in terms of computational speed and flexibility.

In this paper, we shall explore another advantage of the new LBE algorithm – its capability to simulate the Navier–Stokes equation with high Reynolds number. It is well understood that the previous LBE method has fundamental difficulties in simulating fluid flows with high Reynolds number [2]. Given the characteristic velocity U, the physical length L, and the viscosity v in a hydrodynamic system, the Reynolds number is defined as

$$R_e = \frac{UL}{v}\,, \tag{1}$$

where v is the viscosity. In the previous LBE models with a lattice mesh of lattice constant δ_x and a sound speed c_s, the Reynolds number can be rewritten as

$$R_e = MN_L R_e^*\,, \tag{2}$$

where $M = U/c_s$ is the Mach number, $N_L = L/\delta_x$ is the number of lattice spacings corresponding to L, and the local Reynolds number R_e^* [3] is defined as

$$R_e^* = \frac{c_s \delta_x}{v}\,. \tag{3}$$

To be concrete, let us take the 9-bit lattice BGK model [4,5] as an example. In this model,

$$c_s = \frac{1}{\sqrt{3}} c\,,$$
$$v = \frac{(2\tau - 1)}{6}\delta_x c\,,$$

where $c = \delta_x/\delta_t$, τ is the dimensionless relaxation time, and δ_t is the time step size. Then, the local Reynolds number for the model is

$$R_e^* = \frac{2\sqrt{3}}{(2\tau - 1)}\,, \tag{4}$$

and the Reynolds number becomes

$$R_e = MN_L \frac{2\sqrt{3}}{(2\tau - 1)}\,. \tag{5}$$

Because the LBE method is based on a small velocity expansion, the Mach number M should be small in principle, and it is usually chosen to be less than 0.15 in practice. There are two options to enhance the Reynolds number in the simulations using the LBE method: One is to reduce the viscosity by decreasing τ toward $\frac{1}{2}$, the other is to increase N_L by enlarging the system size of the mesh. It is well known that the system becomes numerically unstable when τ is close to $\frac{1}{2}$. This precludes the possibility of

enhancing R_e^* via setting τ close to $\frac{1}{2}$, and thus we must enlarge the system size in order to enhance the Reynolds number significantly. (How close τ can be to $\frac{1}{2}$ is case-dependent.) This illustrates how difficult it is for the LBE method to simulate the incompressible Navier–Stokes equation with high Reynolds number. The difficulty is twofold: One is the very basis of the LBE method – the small velocity expansion of the equilibrium distribution function around zero velocity, which sets the fundamental limit on the Reynolds number. The other is the uniformity of the lattice mesh associated with previous LBE models, which reduces the efficiency and effectiveness of the LBE method enormously. Currently available numerical results [6–8] have shown that the mesh sizes of the simulations using the LBE method are usually much larger than that of simulations using conventional numerical methods, such as finite difference or finite element, for identical problems.

In this paper, we show that the LBE algorithm with arbitrary and nonuniform mesh grids is also capable of simulating high Reynolds number hydrodynamics with a mesh size much smaller than that in previous LBE algorithms. With the new LBE algorithm, the mesh size in a simulation is determined by the underlying physics, or the Reynolds number. In other words, the mesh size is determined by the resolution needed for the smallest scale in the flow motion of the system.

This paper is organized as follows: Section 2 gives the theoretical justification for using the LBE method with nonuniform mesh grids to simulate the Navier–Stokes equation with high Reynolds number. Section 3 provides numerical results of simulations of flow in a 2-D sudden expansion channel by using the new LBE algorithm with nonuniform mesh grids. Section 4 discusses the results and concludes the paper.

2. Theory

The evolution process of the new LBE algorithm [1] has three steps: collision, advection, and interpolation. The collision and advection processes are identical to that in the previous LBE algorithms. Thus, the only distinction of the new LBE algorithm from other LBE algorithms is the interpolation process used in the new algorithm. The justification for using interpolation in the LBE method is that the distribution functions, either f_α (the single-particle distribution) or p_α (the pressure distribution), are smooth continuous functions in both space and time. Furthermore, interpolation does not compromise the accuracy of the LBE method so long as the accuracy of the interpolation scheme has an accuracy of the second order (in space) or higher. Not only does the new algorithm retain all the advantages of the LBE method, but also it greatly enhances the computational efficiency of the LBE method, because the mesh size can be much reduced without sacrificing accuracy in the LBE algorithm.

The key idea in constructing the new LBE algorithm with arbitrary mesh grids is that the mesh grid size can be distinguished and thus separated from the lattice constant of the lattice mesh, which is also the minimum distance "particles" are allowed to advect with a given time step. That is to say, the spatial discretization can be completely

separated from the discretization in the velocity space. Let us restrict ourselves to a uniform rectangular mesh without loss of generality. The ratios between the grid size of the rectangular mesh dX or dY and the lattice constant δ_x or δ_y are

$$r_x = \frac{dX}{\delta_x}, \qquad r_y = \frac{dY}{\delta_y}. \tag{6}$$

The local Reynolds number associated with the new mesh is

$$R_e^* = \frac{rc_s\delta}{\nu}, \tag{7}$$

where r and δ denote r_x or r_y and δ_x or δ_y, whichever is appropriate. Thus, the Reynolds number can be increased r-fold in the new algorithm without changing the values of c_s, ν, and δ. This suggests that it is not necessary to reduce the value of τ to enhance the Reynolds number, provided that the resolution determined by the mesh grids is sufficient for the given Reynolds number. Therefore, increasing the Reynolds number can be achieved without affecting the stability of the system.

3. Numerical results

All of our numerical simulations were computed on IBM RISC/6000 590 workstations at Los Alamos National Laboratory, with double precision (64 bits).

3.1. The details of the simulation

In this paper, the flow in a 2-D symmetric channel with sudden expansion is studied using the 9-bit LBE model for the incompressible Navier–Stokes equation [5]. Non-slip boundary conditions [9] are applied at the walls of the channel. At the entry of the channel a parabolic profile of u_x with a maximum $U_0 = 0.1c$ is enforced. At the exit, the boundary condition of a constant pressure,

$$p(x = N_x, t) = 1.0\rho_0 c^2,$$

is applied. The second-order upwind interpolation is used in the interior of the channel and the second-order central difference interpolation is applied to the mesh grids next to boundaries.

The geometric configuration of the channel is set as follows. The expansion ratio is 1:3, and the aspect ratio of the channel is 1:8 or 1:20 depending on the Reynolds number. The Reynolds number of the system is defined as

$$R_e = \frac{hU_0}{2\nu},$$

where h is the height of the entry, and U_0 the maximum velocity at the entry. A section of the entrance channel of length $h/2$ and h is included in the simulations for $R_e = 60$ and 140, respectively.

The meshes used in the simulation are uniform rectangular ones. The rectangular mesh grids in the meshes have an aspect ratio of 2 : 1, i.e., $r_x : r_y = 2 : 1$ for all meshes.

In order to compare the results of our simulation with the up-to-date experimental data and numerical results in Ref. [10], the calculations corresponding to $R_e = 26$, 60, and 140 were performed. The flow is nominally two-dimensional and steady with $R_e \leqslant 140$ [10]. For $R_e = 26$ and 60, the mesh size of the channel (excluding the entrance section) is $N_x \times N_y = 193 \times 49$, and for $R_e = 140$, the mesh size is $N_x \times N_y = 481 \times 49$. It is ensured that the channel length is long enough to allow flow to be fully developed at the exit for the chosen values of R_e.

With the above arrangement of the channel configuration, and using the 9-bit LBE model for the incompressible Navier–Stokes equation [5], the Reynolds number of the system is

$$R_e = \frac{4.8 r_y}{(2\tau - 1)} . \tag{8}$$

In our simulations, the Reynolds number is varied by adjusting both r_y and τ.

3.2. Results of the simulation

The results shown in what follows are the contour lines of the stream function, $\psi(x, y)$, and the velocity profiles of the horizontal velocity, $u_x(x, y)$, at several sections of the channel. The results are directly compared with the experimental results in Ref. [10]. The stream function of the flow is defined as

$$\psi(x, y) = \int_{y=-1.5h}^{y} u_x(x, y')\, dy' , \tag{9}$$

where $y/h = -1.5$ is set along the lower wall of the channel.

3.2.1. $R_e = 26$

At $R_e = 26$, the flow is symmetric about the centerline of the channel. The mesh size is 193×49, and two values of r_y, 1 and 8, are chosen in the simulation. With given $R_e = 26$ and r_y, the values of τ, determined by Eq. (8), are 0.5923 and 1.2385, for $r_y = 1$ and 8, respectively.

Fig. 1 shows the contour lines of the stream function, ψ, obtained with (a) $r_y = 1$, and (b) $r_y = 8$, respectively. The pattern of ψ is symmetric about the centerline of the channel, as expected. The contour lines obtained with both $r_y = 1$ and $r_y = 8$ are very much the same.

Fig. 2 shows the velocity profile of horizontal velocity, u_x, at two sections of the channel, $x/h = 2.5$ and 5.0, respectively. Experimental data in Ref. [10] are also included in the same figure.

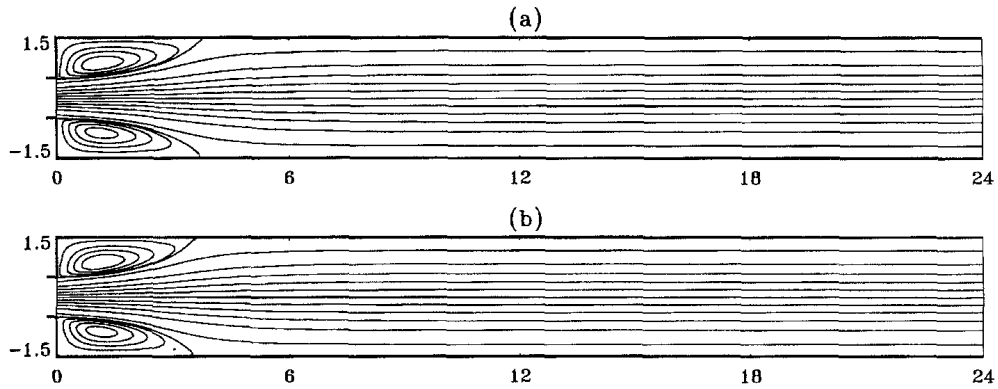

Fig. 1. The contour lines of the stream function ψ for the flow at $R_e = 26$: (a) $r_y = 1$ ($\tau = 0.5923$), (b) $r_y = 8$ ($\tau = 1.2385$).

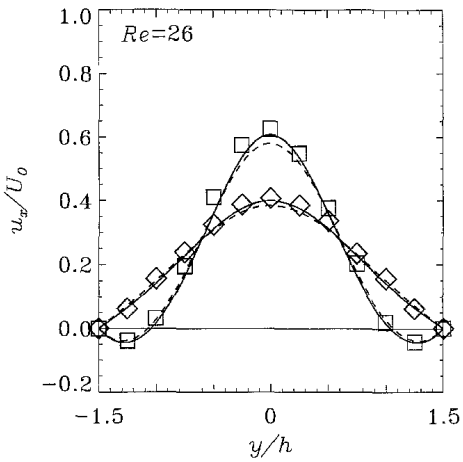

Fig. 2. The velocity profile of u_x for the flow at $R_e = 26$. The solid lines and dashed lines represent the results with $r_y = 1$ and $r_y = 8$, respectively. The profiles are sampled at $x/h = 2.5$ and 5.0. Symbols □ and ◇ represent the experimental data in Ref. [10] sampled at $x/h = 2.5$ and 5.0, respectively.

3.2.2. $R_e = 60$

At $R_e = 60$, the flow is asymmetric about the centerline of the channel. The mesh size is the same as in the previous case, 193×49. Two values of r_y, 2 and 8, are chosen in the simulation.

Fig. 3 shows ψ at $R_e = 60$. Similar to Fig. 1, Fig. 3 shows ψ obtained with (a) $r_y = 2$ ($\tau = 0.58$), and (b) $r_y = 8$ ($\tau = 0.82$). The flow at $R_e = 60$ is clearly asymmetric.

Fig. 4 shows u_x at two sections of the channel, $x/h = 2.5$ and 5.0, respectively. Experimental data in Ref. [10] are also presented in the same figure.

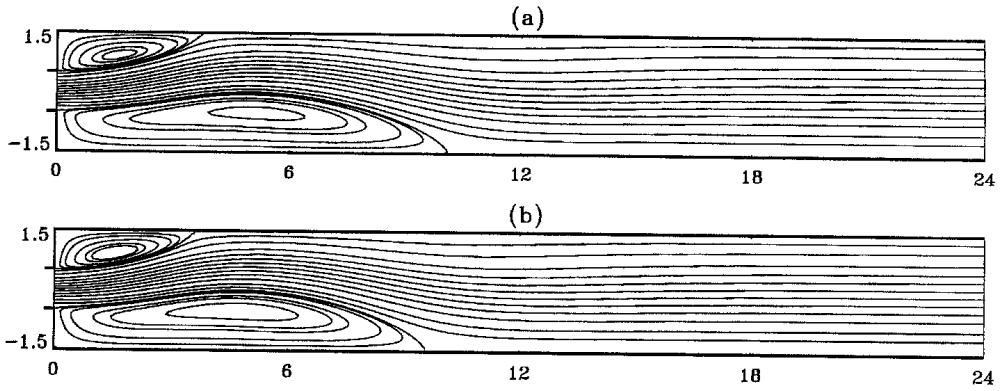

Fig. 3. The contour lines of the stream function ψ for the flow at $R_e = 60$: (a) $r_y = 2$ ($\tau = 0.58$), (b) $r_y = 8$ ($\tau = 0.82$).

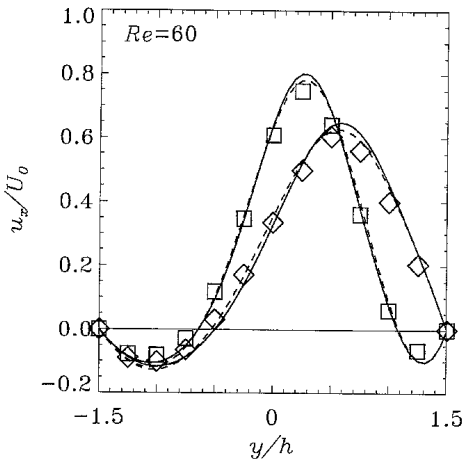

Fig. 4. The velocity profile of u_x for the flow at $R_e = 60$. The solid lines and dashed lines represent the results with $r_y = 2$ and $r_y = 8$, respectively. The profiles are sampled at $x/h = 2.5$ and 5.0. Symbols □ and ◇ represent the experimental data in Ref. [10] sampled at $x/h = 2.5$ and 5.0, respectively.

3.2.3. $R_e = 140$

For $R_e = 140$, the mesh size is chosen to be 481×49 (aspect 1 : 20) to ensure that the flow is fully developed downstream of the channel. At $R_e = 140$, the flow is not only asymmetric, a third recirculation area has also developed downstream and on the same wall as the smaller recirculation region near the entrance.

Fig. 5 shows ψ at $R_e = 140$ with (a) $r_y = 4$ ($\tau \approx 0.5686$), and (b) $r_y = 8$ ($\tau \approx 0.6371$). The figure clearly displays the third recirculation region. The location of this recirculating region in our simulation is very close to both experimental and numerical results in Ref. [10].

Fig. 6 shows u_x at two sections of the channel, $x/h = 2.5$ and 20.0, respectively. The results are compared with the experimental data in Ref. [10].

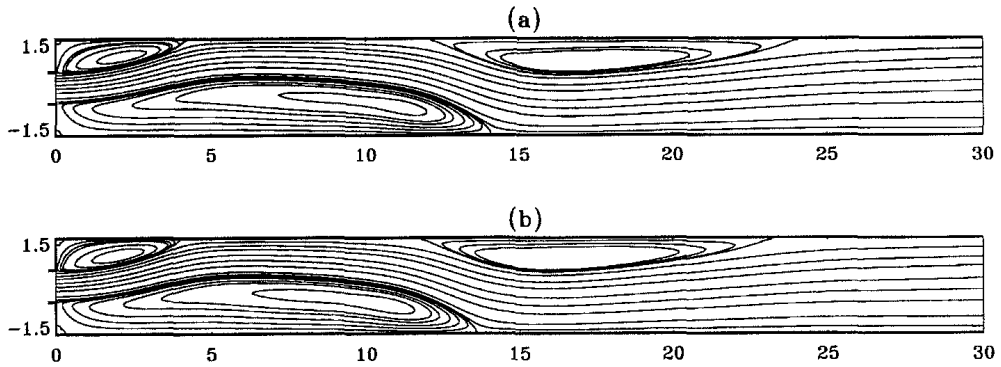

Fig. 5. The contour lines of the stream function ψ for the flow at $R_e = 140$: (a) $r_y = 4$ ($\tau = 0.5686$), (b) $r_y = 8$ ($\tau = 0.6371$).

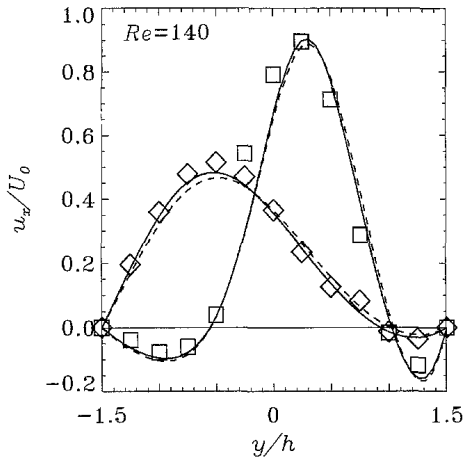

Fig. 6. The velocity profile of u_x for the flow at $R_e = 140$. The solid lines and dashed lines represent the results with $r_y = 4$ and $r_y = 8$, respectively. The profiles are sampled at $x/h = 2.5$ and 20.0. Symbols □ and ◇ represent the experimental data in Ref. [10] sampled at $x/h = 2.5$ and 20.0, respectively.

3.2.4. *Effect of the ratio r*

In the above three cases, the results with different values of r (or τ) for the same value of the Reynolds number all demonstrate a quantitative consistency among them. Table 1 shows the relative difference of the velocity fields:

$$\|\delta \boldsymbol{u}(t)\| = \frac{\sum_i \|(\boldsymbol{u}_1(\boldsymbol{x}_i, t) - \boldsymbol{u}_2(\boldsymbol{x}_i, t))\|}{\sum_i \|(\boldsymbol{u}_2(\boldsymbol{x}_i, t)\|}, \tag{10}$$

where $\|\cdot\|$ denotes the L_2 norm, and the sum is over the entire system. As shown in Table 1, the highest relative global difference, which is about 4%, occurs in the case of $R_e = 140$.

All of our numerical results are in good agreement with the experimental data as well as the numerical results of Ref. [10].

Table 1
The relative global difference of the velocity fields obtained with different values of r_x, defined by Eq. (10), for the simulations of the flow in 2-D symmetric channel with expansion

R_e	r_x's	$\|\delta u(t)\|$ (%)
26	1, 8	1.29
60	2, 8	3.95
140	4, 8	3.99

4. Conclusion and discussion

In this paper, we have successfully demonstrated that the LBE method is indeed capable of simulating flows with high Reynolds number without the lattice Reynolds number limitation of previous LBE models. The limitation of the Reynolds number in the new LBE algorithm is now set by the resolution of the mesh, like other conventional methods of computational fluid dynamics (CFD). Therefore, the barrier to enhancing Reynolds number in previous LBE models has been overcome.

The key idea of the new algorithm is to distinguish and thus separate the advection step size, δ_x (or δ_y), and the grid size, dX (or dY). By increasing the ratio between the advection step size and the grid size, the Reynolds number is enhanced while the grid size and the value of τ remain unchanged. In other words, the value of τ is increased while both the Reynolds number R_e and the grid size remain unchanged. This certainly improves the stability of the LBE method.

It should be emphasized that interpolations used in the new LBE algorithm do not degrade the accuracy of the LBE algorithm itself. This point has been made in our previous report [1], and it is demonstrated again in the present simulation.

The results of our simulations of the flow in the sudden expansion channel are satisfactory and in good agreement with previous experimental as well as numerical results.

With the improvement of arbitrary mesh grids and the Reynolds number enhancement made here, the LBE method can be a superior computational method in CFD because of its virtues: algorithmic parallelism, programming simplicity, and the ease with which interactions can be incorporated in the models.

Acknowledgements

The authors would like to thank Dr. Gary Doolen for his support and encouragement during this work. The editorial assistance of Mr. David V. Brydon is gratefully acknowledged.

References

[1] X. He, L.-S. Luo and M. Dembo, Some progress in lattice Boltzmann method: Part I. Nonuniform mesh grids, J. Comput. Phys., 129 (1996) 357.
[2] S.A. Orszag and V. Yakhot, Reynolds number scaling of cellular automata hydrodynamics, Phys. Rev. Lett. 56 (1986) 1691. Although this reference discusses the Reynolds number scaling of cellular automata hydrodynamics, the discussion related to the small Mach number limitation is valid for LBE as well.
[3] U. Frisch, D. d'Humières, B. Hasslacher, P. Lallemand, Yv. Pomeau and J.-P. Rivet, Lattice gas hydrodynamics in two and three dimensions, Complex Systems 1 (1987) 649.
[4] Y.H. Qian, D. d'Humières and P. Lallemand, Lattice BGK models for the Navier–Stokes equation, Europhys. Lett. 17 (1992) 479.
[5] X. He and L.-S. Luo, Lattice Boltzmann model for the incompressible Navier–Stokes equation, J. Stat. Phys., in press.
[6] L.-S. Luo, Lattice-gas automata and lattice Boltzmann equations for two-dimensional hydrodynamics, Ph.D. Thesis, Georgia Institute of Technology, Atlanta (1993).
[7] S. Hou, Q. Zou, S. Chen, G. Doolen and A.C. Cogley, Simulation of cavity flow by the lattice Boltzmann method, J. Comput. Phys. 118 (1995) 329.
[8] L.-S. Luo, Symmetry breaking of flow in 2-D symmetric channels: simulations by lattice Boltzmann method, Int. J. Mod. Phys. C, in press.
[9] X. He, Q. Zou, L.-S. Luo and M. Dembo, Analytic solutions of simple flows and analysis of non-slip boundary conditions for the lattice Boltzmann BGK model, J. Stat. Phys., in press.
[10] R.M. Fearn, T. Mullin and K.A. Cliffe, Nonlinear flow phenomena in a symmetric sudden expansion, J. Fluid Mech. 211 (1990) 595.